Efficient Removal of a Toxic Textile Dye from Aqueous Solution using Low-Cost Adsorbents Natural Clays

Younes Rachdi[1], Marouane El Alouani[2], Rajaa Bassam[1], El Hassane Mourid[3], Az-iddin Chham[4], Hamid Saufi[2], El Hassan El Khattabi[1], El Hassane Khouya[1] and Said Belaaouad[1]

[1]Laboratory of Physical Chemistry of Materials LCPM, Faculty of Sciences Ben M'Sik, Hassan II University of Casablanca, B.P.7955, Bd Cdt Driss El Harti, Casablanca, Morocco

[2]Laboratory of Physico-Chemistry of Inorganic and Organic Materials (LPCIOM), Materials Science Centre (MSC), Mohammed V University, Ecole Normale Superieure (ENS), Rabat, Morocco

[3]Physical Chemistry of Materials Team, Cadi Ayyad University, Marrakech, Morocco

[4]Laboratory of Organic Synthesis, Extraction and Valorization, Faculty of Sciences Aïn Chock Hassan II University, B5366, Casablanca 20000, Morocco

*Corresponding author (e-mail: rachdi.smc@gmail.com)

The objective of this work was to study the capacity of raw Moroccan clays in removing an organic micropollutant, methylene blue (MB), from an aqueous environment. The chemical composition, mineralogical phase, surface functional groups and surface morphology of the adsorbents used were examined using X-ray Fluorescence (XRF), X-ray diffraction (XRD), Fourier transform infrared spectroscopy (FTIR) and scanning electron microscope (SEM) techniques. Experimental factors influencing adsorption such as adsorbent mass, initial pH of the solution, adsorbate initial concentration, adsorbent-adsorbate contact time as well as temperature were investigated. The kinetic study showed that the adsorption process was explained by a pseudo-second-order reaction and the contact time was 30, 45 and 60 min respectively for Red Clay (RC), Green Clay (GC), and White Clay (WC) samples. The isotherm data showed that the Langmuir model was most appropriate to describe the adsorption of MB by the three samples. The maximum adsorption capacities obtained using the Langmuir model were 50.47, 32.57, and 16.78 mg g^{-1} respectively for RC, GC, and WC. The thermodynamic parameters indicated that MB adsorption onto all clays was endothermic and spontaneous. The regeneration study showed that the adsorbents used were recyclable but showed a decrease of their adsorption capacity. Therefore, RC, GC and WC could be used for the treatment of wastewater contaminated by MB and similar organic compounds.

Keywords: Adsorption; Moroccan clay; regeneration; methylene blue

Received: February 2023; Accepted: March 2023

Water resources are greatly reduced following a demographic increase accompanied by strong industrialisation and intensive development of agriculture [1,2]. The amount of micropollutants, particularly dyes, in the environment are constantly increasing [3]. In general, these pollutants are toxic, non-degradable and cause numerous harmful effects on human health.

The toxicity of a dye depends on its chemical composition, structure and its concentration in wastewater. Methylene blue (MB), a dye commonly used for dyeing wood and cotton [4], can cause skin irritation, stomach disorders, eczema, and respiratory difficulties [5].

Several processes are used to remove dyes from wastewater, such as adsorption, coagulation-flocculation, advanced oxidation, electrochemical treatment and biological treatment [6, 7]. Adsorption using various commercial, natural and synthetic adsorbents, is one of the most effective processes for the removal of dyes [8, 13].

Clay minerals have a high adsorption capacity for dyes due to their specific physico-chemical properties such as high porosity, high specific surface area, and high cation exchange capacity[14]. Numerous studies in the literature have investigated the retention of dyes from aqueous solution using clays [15,16]. In a study by Bentahar, the adsorption of methylene blue from an aqueous medium was effected using red clay and ghassoul [15]. In another study, Elmoubarki investigated the retention of textitle dyes onto raw clays sampled from Morocco [2].

The objective of the present study was to evaluate the performance of three natural clays collected from Morocco in the elimination of MB from aqueous solution. The parameters investigated included adsorbent mass, contact time, solution pH, temperature and initial MB concentration. Pseudo-first order (PFO), pseudo-second-order (PSO), and intra-particle diffusion (IPD) models were applied to evaluate the kinetic study. The equilibrium data were analyzed using Langmuir and Freundlich models. The

thermodynamic study also was evaluated and discussed. The desorption of MB was performed using a thermal method.

MATERIALS AND METHODS

1. Materials

Three natural clay samples were collected from two different sites in Morocco (Figure 1). The red clay (RC) and green clay (GC) samples were collected from the Sidi Moussa El Mejdoub region located 10 km east of the city of Mohammed (site A), while the white clay (WC) sample was collected from the Ain Dorij region located 47 km east of the city of Ouezzane (site B). The RC, GC and WC samples were crushed and then sieved using a Retsch Tamiseuse AS 300 control (Germany) sieve shaker to obtain particles with a diameter of less than 200 µm.

MB is a cationic dye with the molecular formula $C_{16}H_{18}ClN_3S$. It is marketed by Riedel de Haen (99% purity, Germany). The choice of this dye as a synthetic pollutant was dictated by its wide use, its toxicity, and its easy detection by UV-visible spectroscopy. The hydrochloric acid (HCl) and sodium hydroxide (NaOH) used were supplied by Sigma-Aldrich ((99% purity, Germany). All solutions were prepared with distilled water using a GFL Gesellschaft Fuer Labortec™ 2108 Water Distiller (Germany).

2. Characterization of the Clay Adsorbents

The chemical composition of the RC, GC and WC samples was analyzed by X-ray Fluorescence (XRF) using a Philips Panalytical PW2400 spectrometer (Netherlands), while mineralogical phase analysis was performed on powdered samples with a BRUKER-BINARY V4 (Germany) diffractometer (XRD) with the following test parameters: 45 kV, 40 mA, and Cu radiation (Kα) with a scan speed of 1°/min from 2θ = 3° to 90° and steps of 2θ = 0.06°. FTIR spectroscopy was used to determine the functional groups on the surface of the RC, GC, and WC samples before and after adsorption using a BRUKER-TENSOR 27 Spectrometer (Germany). The surface morphology of the samples before and after adsorption was analyzed by scanning electron microscopy (SEM) using a HIROX model SH 4000M (Germany). pH values were measured with an APERA PH820 (China) pH meter. The point of zero charge (PZC) was identified by the drift method [17], and the cation exchange capacity (CEC) was determined by the hexamine-cobalt method [18].

3. Batch Equilibrium Studies

The adsorption experiments were carried out to study the parameters influencing the adsorption of MB by RC, GC and WC, such as the initial pH of the solution, the initial concentration of the adsorbate, the dose of adsorbent, the temperature, and the adsorbent-adsorbate contact time.

50 mL of MB solutions with initial concentrations of 100 $mg.L^{-1}$ were placed in three Erlenmeyer flasks (250 mL). Equal masses of 0.1 g, 0.2 g and 0.3 g respectively of the RC, GC and WC clays with a particle size of 200 µm were added to each flask and the mixture was stirred at 450 rpm in an isothermal room at 25 °C for 2 h to reach equilibrium.

Figure 1. Topographic map of the collection sites of RC, GC, and WC: The RC and GC were collected from site A and the WC from site B.

The initial pH of the adsorbate solution was adjusted by adding HCl (0.1 M) or NaOH (0.1 M). At the end of each test, an aqueous sample was taken from the final solution. Before analysis, all samples were centrifuged at 3000 rpm for 10 min to minimize interference due to the presence of suspended clay particles. The MB concentration of each solution was measured at 664 nm using a double beam Rayleigh Beifen-Ruili Analytical Model UV1800 UV/VIS spectrophotometer (China). Similar procedures were followed for each clay adsorbent under different conditions.

The amount of MB adsorbed was determined using the following equation:

$$Q = \frac{(C_0 - C)V}{m} \quad (1)$$

where Q ($mg.g^{-1}$) is the quantity of pollutant adsorbed per unit mass of the adsorbent, C and C_0 ($mg.L^{-1}$) are the concentrations of MB after and before adsorption, respectively, V (L) is the volume of MB solution, and m (g) is the amount of the clay.

3.1. Kinetic Study

The study of adsorption kinetics is essential to determine the adsorption mechanism. The kinetics of MB adsorption by RC, GC and WC were studied using different kinetic models: pseudo-first-order, pseudo-second-order and intra-particle diffusion [19].

The general linear expression of the pseudo-first-order model presented by Lagergren [19], is given by the following equation:

$$\ln(Q_e - Q_t) = \ln(Q_e) - K_1 t \quad (2)$$

where Q_t and Q_e ($mg.g^{-1}$) are the quantity adsorbed at time t and equilibrium, respectively, and K_1 (min^{-1}) is the pseudo-first-order adsorption rate constant.

The general linear expression of the pseudo-second-order model is [19] :

$$\frac{t}{Q_t} = \frac{1}{Q_e} t + \frac{1}{K_2 Q_e^2} \quad (3)$$

where K_2 ($g.mg^{-1}.min^{-1}$) is the pseudo-second-order constant [19].

The general linear expression of the intra-particle diffusion kinetic model is expressed by the equation [19]:

$$Q_t = K_3 t^{0,5} + C \quad (4)$$

where K_3 ($mg.g^{-1}\ min^{-0,5}$) is the intraparticle diffusion rate constant and C ($mg.g^{-1}$) is a constant which gives information on the thickness of the limit layer.

3.2. Isotherm Study

The adsorption isotherm is important to explain the mechanism of the adsorbent-adsorbate interaction at equilibrium [5]. Several models of adsorption isotherms are given in the literature. In this work, the experimental results were evaluated using the Langmuir and Freundlich isotherm equations [19].

The general linear expression of the model developed by Langmuir is given by the equation :

$$\frac{C_e}{Q_e} = \frac{1}{K_L . Q_{max}} + \frac{C_e}{Q_{max}} \quad (5)$$

where K_L ($L.mg^{-1}$) is the Langmuir constant, Q_{max} ($mg.g^{-1}$) is the maximum quantity of solute adsorbed and C_e ($mg.L^{-1}$) is the concentration of pollutants at equilibrium.

The general linear expression of the model developed by Freundlich is given by the equation:

$$\ln Q = \frac{1}{n} \ln C_e + \ln K_F \quad (6)$$

where K_f is the Freundlich constant which expresses the adsorption affinity, and 1/n is another constant that expresses the intensity of the adsorption.

3.3. Thermodynamic Study

Thermodynamic data can be used to determine the influence of temperature on the adsorption process and to estimate the nature of the adsorption [4]. The influence of temperature on the retention of MB by RC, GC and WC was studied by varying the temperature from 25 to 45 °C, with the other parameters constant (initial concentration 100 $mg.L^{-1}$, adsorbate mass of 0.1 g, 0.2 g, and 0.3 g respectively for RC, GC, and WC). The parameters such as free energy ΔG° ($J.mole^{-1}.K^{-1}$), enthalpy ΔH° ($KJ.mole^{-1}$), and entropy ΔS° ($J.mole^{-1}.K^{-1}$), can be determined by the following equations [19]:

$$\Delta G^\circ = -RT \ln K_D \quad (7)$$

$$K_D = \frac{Q_e}{C_e} \quad (8)$$

$$\ln K_D = \frac{\Delta S^\circ}{R} - \frac{\Delta H}{RT} \quad (9)$$

where R is the universal perfect gas constant (R =8.314 J.mol^{-1}.K^{-1}), T(K) is the absolute solution temperature, K_d is the distribution coefficient.

3.4. Regeneration Study

Regeneration of adsorbents is important to conserve natural resources. In this study, the RC, GC and WC were thermally regenerated after MB adsorption using a Protherm L-012K2EN Muffle Furnace (Germany), at a temperature of 400 °C for 2 h. The percentage of MB removal by the regenerated RC, GC and WC samples was determined using a 100 mg.L^{-1} MB solution stirred at 450 rpm for 2 h at room temperature. The adsorbents were regenerated and reused 5 times.

RESULTS AND DISCUSSION

1. Characterization of the Clays

1.1. XRF Analysis

The chemical composition of RC, GC and WC as obtained by XRF analysis is presented in Table 1. The results indicate that RC was mainly composed of SiO_2, Fe_2O_3, Al_2O_3, MgO, and CaO, which represented 95.21% of the total mass, while the GC consisted of SiO_2, Al_2O_3, MgO, and CaO (91.72 %). The WC contained 77.5% SiO_2 and CaO. The RC, GC and WC samples also contained traces of sodium, potassium and other elements. The large percentage of SiO_2 and Al_2O_3 showed that the RC and GC were aluminosilicates.

Table 1. Mineral composition of RC, GC and WC.

Component (%)	Na_2O	Al_2O_3	SiO_2	Fe_2O_3	K_2O	MgO	CaO	Other
RC	0.383	7.658	59.274	11.266	3.126	6.319	10.695	1,279
GC	0.287	18.981	53.317	3.478	1.361	8.581	10.843	3,152
WC	0.493	3.82	61.456	5.827	0.758	5.110	15.701	6.835

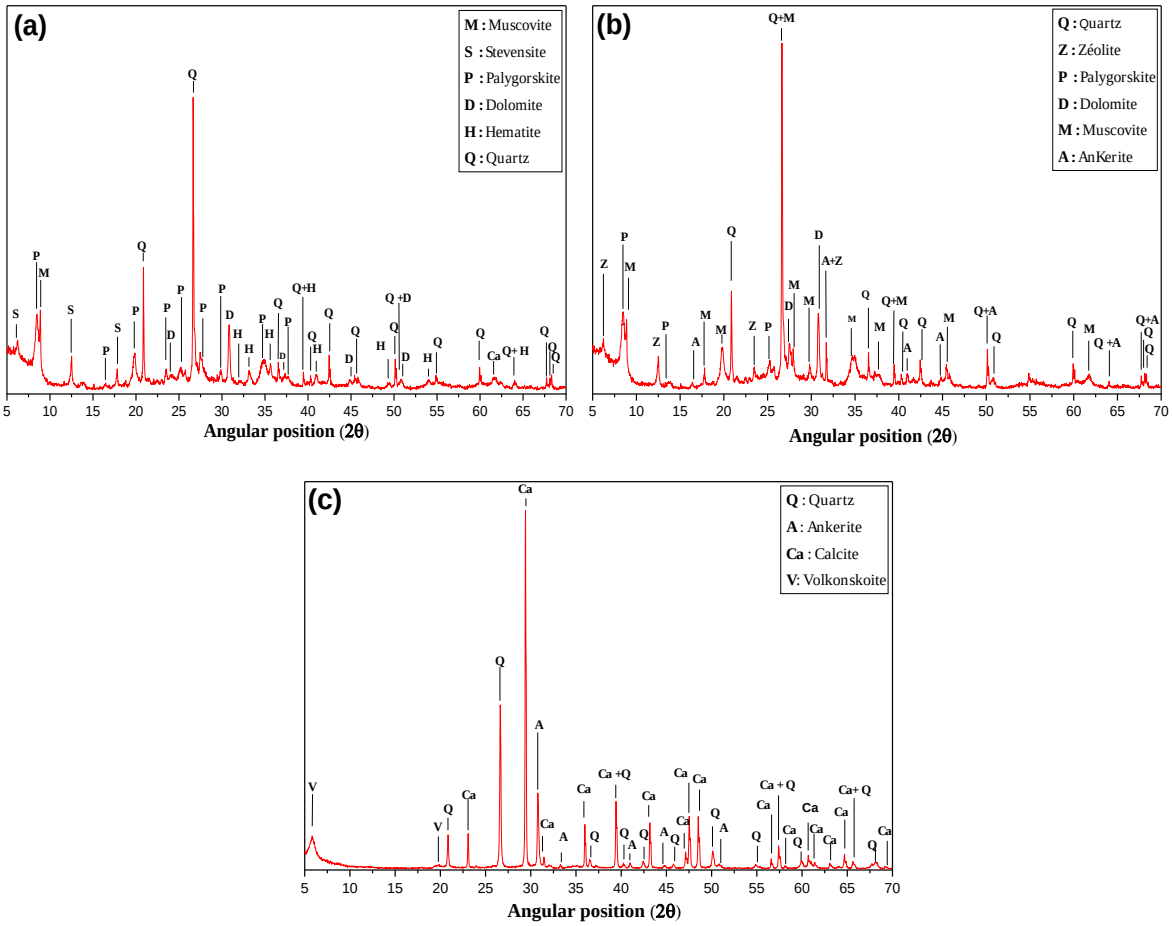

Figure 2. XRD patterns of (a) RC, (b) GC and (c) WC.

1.2. XRD Analysis

The X-ray diffractograms of RC, GC and WC are presented in Figure 2. The results indicate that RC was composed mainly of quartz, hematite, dolomite, muscovite, palygorskite, ankerite, and stevensite. The GC sample was composed of quartz, muscovite, palygorskite, ankerite, dolomite, and zeolite, while WC contained quartz, calcite, ankerite and volkonskoite.

1.3. FTIR Analysis

The FTIR spectra of RC, GC and WC before and after MB adsorption are presented in Figure 3. The FTIR spectra of RC and GC before adsorption showed bands around 3614 cm^{-1} corresponding to the stretching of M-OH (M: Mg, Al, Fe) [20]. The bands around 3544 and 3425 cm^{-1} can be attributed to the H-O-H stretching vibration of hydrated water [21]. The CO_2 peak appeared at 2358 cm^{-1} [22]. The band at 1658 cm^{-1} corresponds to the -OH stretching vibration of water [23]. The peaks at 1026, 784 676, 524, and 464 cm^{-1} were attributed to the Si-O [24] and Si-O-Al stretching vibrations [23]. The bands that appeared between 784 and 532 cm^{-1} correspond to the stretching vibration of Si-O-Al [23]. The peak at 464 cm^{-1} was explained by the bending vibration of Si-O-Si [25]. After adsorption, the appearance of a peak at 1396 cm^{-1} denotes the presence of C-N-C [26], and another at 1540 cm^{-1} was explained by the stretching vibration of C=C [27], which confirms the adsorption of MB by RC. After adsorption onto GC, the bands at 1450 cm^{-1} can be attributed to the (C=C) vibration of the aromatic rings [28], and the bands related to -C=C and -C=N- stretching in polyheterocycles around 1608 cm^{-1} and -C-N- stretching around 1350 cm^{-1} were detected [29], which confirms the retention of MB by GC. For WC, the band around 1436 cm^{-1} corresponds to the torsional vibrations of O-C-O [30], and the band at 873 cm^{-1} is attributed to $CaCO_3$ [31]. The band around 1610 cm^{-1} that appeared after adsorption corresponds to the -C=C and -C=N- stretching in polyheterocycles [32] which indicates the adsorption of MB by WC.

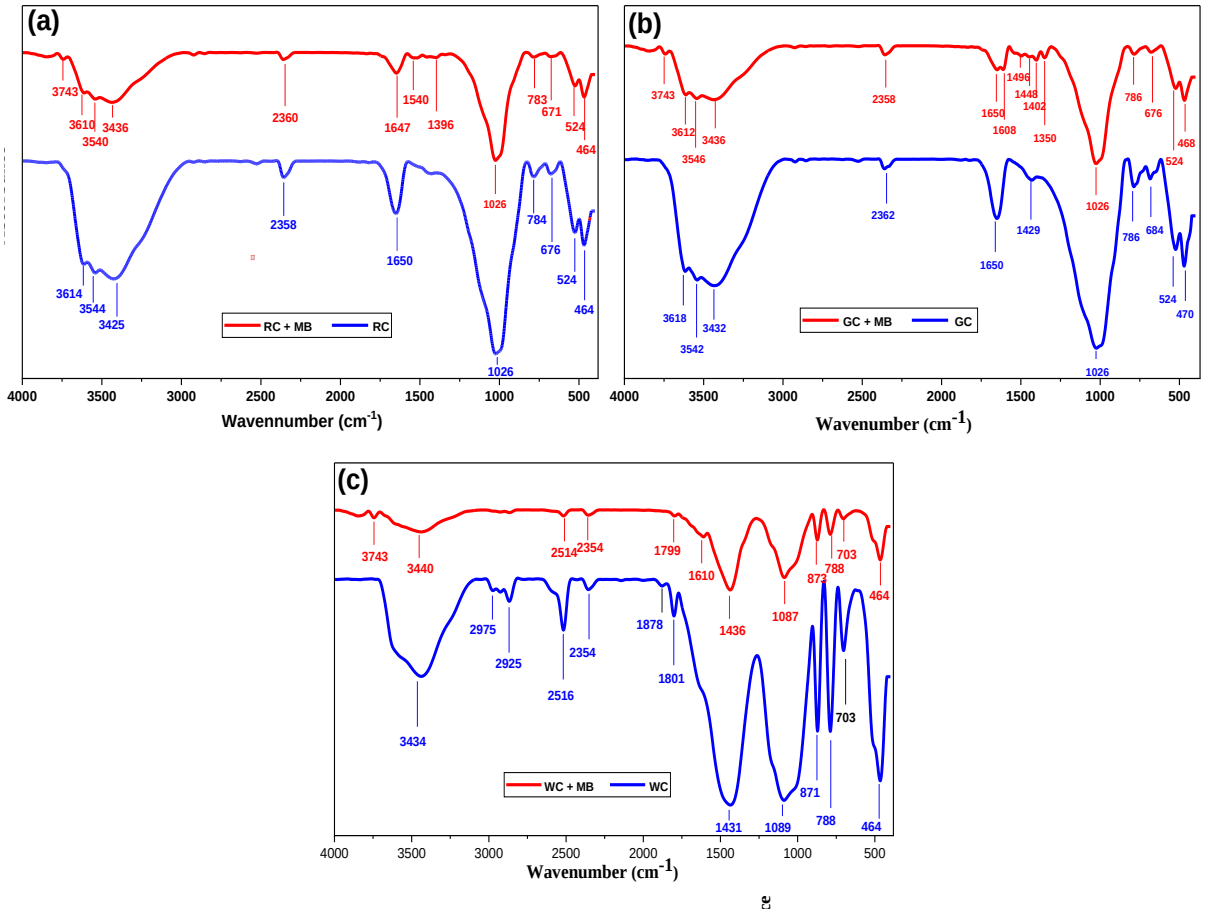

Figure 3. FT-IR spectra before and after MB adsorption by (a) RC, (b) GC, and (c) WC.

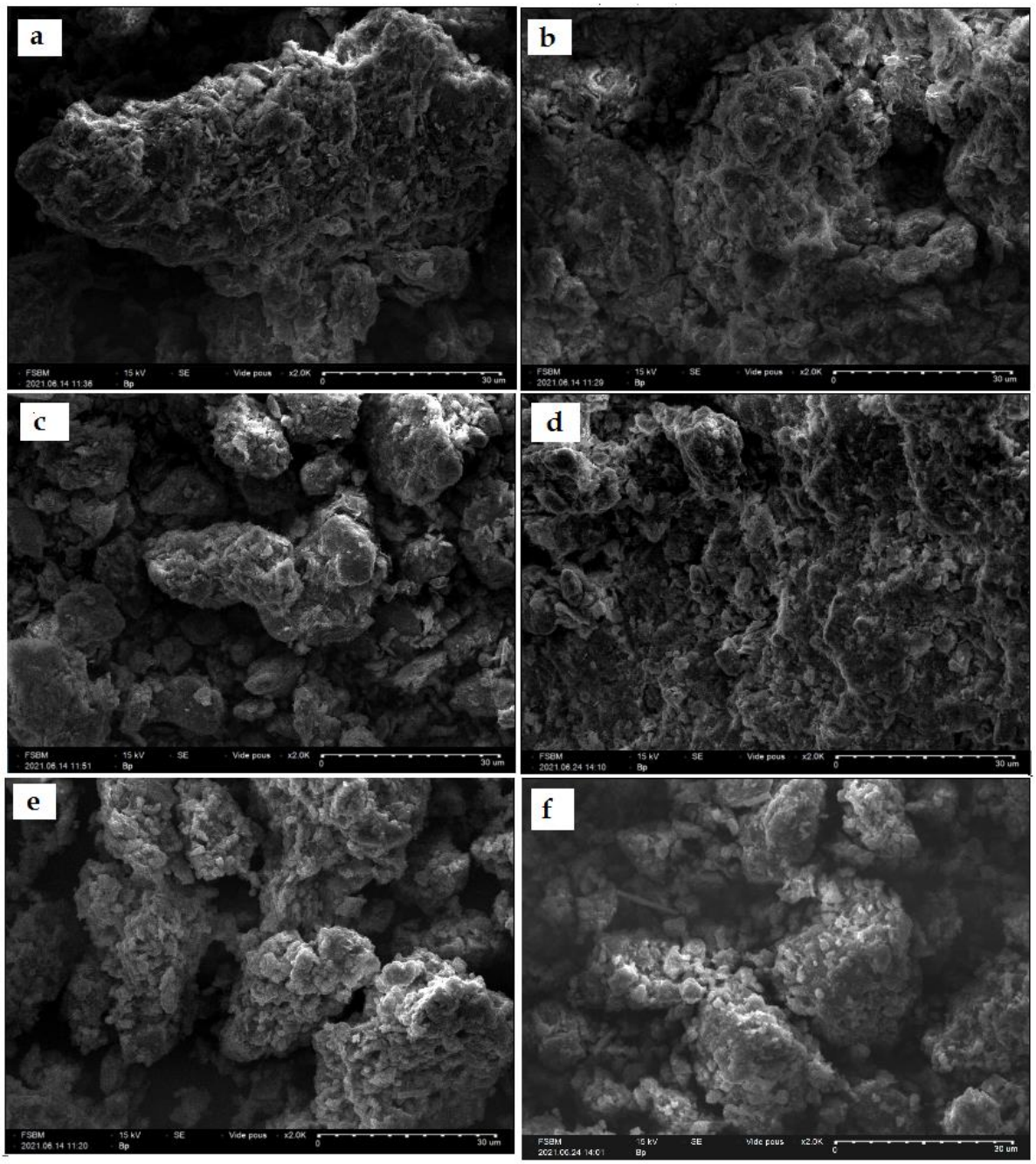

Figure 4. SEM micrographs of (a) RC, (b) RC+MB, (c) GC, (d) GC+MB, (e) WC and (f) WC+MB.

1.4. SEM Analysis

The morphological images of RC, GC, and WC before and after adsorption are depicted in Figure 4. The SEM images before adsorption showed that the samples were irregularly-shaped particles having a homogeneous texture of aggregates with pores and cavities in their structures [33]. The morphologies of RC and GC were similar because they were collected at the same sites. After adsorption, the surface of the RC, GC and WC samples became less porous, showing that MB was well-adsorbed on all three clays.

1.5. PZC and CEC

The PZC is an important parameter to understand the influence of pH on adsorption; it represents the pH where the overall charge of the adsorbent surface is zero. The PZC allows one to determine the charge of the surface as a function of the pH value. When pH<PZC the surface of the solid has a positive charge, and when pH>PZC, the surface becomes negatively charged [34]. Figure 5 shows the PZC values for RC, GC and WC. It can be seen that the PZC values for RC, GC and WC were 7.5, 8, and 8.9 respectively. The PZC curves obtained

for RC, GC, and WC are similar to those reported in earlier studies [19,28]. The CEC values obtained for RC, GC and WC were 85, 79, and 20 meq/100g, respectively.

2. Adsorption Study

2.1. Effect of RC, GC, and WC Mass

The influence of the mass of RC, GC and WC on the retention of MB was tested by varying the adsorbent dose from 0.25 to 10 $g.L^{-1}$, while the other parameters such as the initial solution pH, initial concentration of MB dye (100 $mg.L^{-1}$), contact time (120 min), and temperature (25 °C) remained constant. The results obtained are presented in Figure 6. When the mass of the adsorbent increased from 0.25 to 10 $g.L^{-1}$, the percentage of MB removed increased from 30 % to 98.28 % for RC, from 29 % to 94 % for GC, and from 12.2 % to 89 % for WC. This result can be explained by the increase in the number of active adsorption sites [35]. For amounts greater than 3 $g.L^{-1}$ for RC and GC, and 4 $g.L^{-1}$ for WC, the percentage adsorption remained constant; this may be due to the decrease in the driving force for mass transfer at low concentrations of dye in solution [36]. Therefore the optimal mass of RC, GC and WC chosen for further studies were 2.4 and 6 $g.L^{-1}$ respectively.

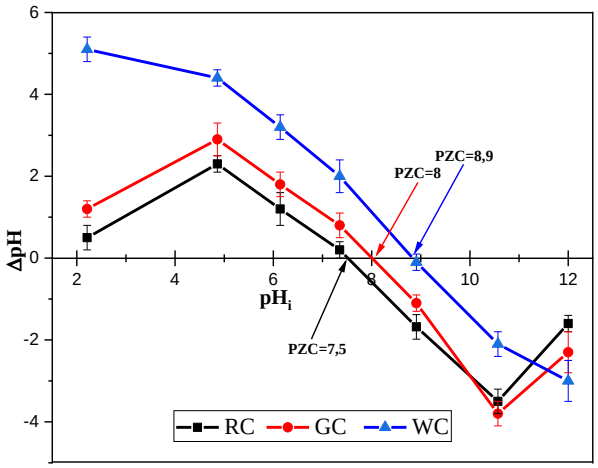

Figure 5. Determination of the PZC of RC, GC and WC.

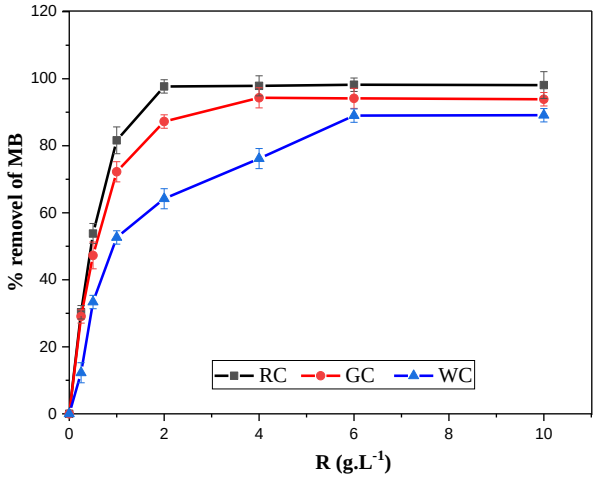

Figure 6. Effect of RC, GC and WC dosage on MB adsorption.

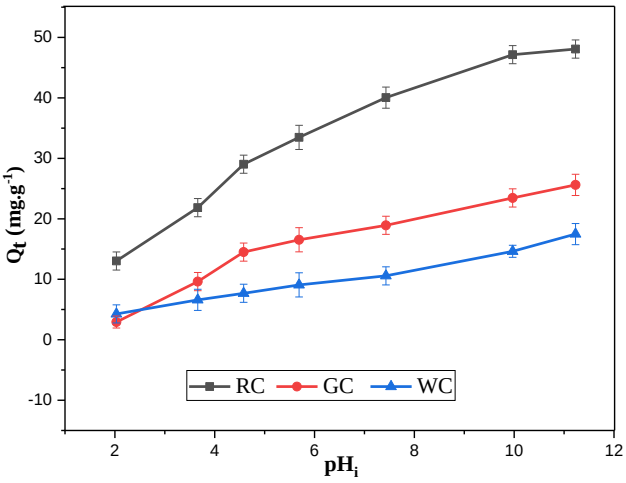

Figure 7. Effect of initial pH on the adsorption of MB by RC, GC, and WC.

2.2. Effect of Initial pH

One of the factors that influenced dye adsorption was the initial pH of the medium. Figure 7 shows the influence of the initial solution pH on the adsorption of MB. The result indicates that the quantity of MB adsorbed by RC, GC and WC increased with increasing pH. To explain this increase it is necessary to determine the PZC of the adsorbent. When pH< PZC, the surface of the adsorbent becomes positively charged, but when pH>PZC it becomes negative. When pH<PZC, the quantity of MB adsorbed by RC, GC and WC was low due to electrostatic repulsion between the positive charge carried by the MB molecule and the positive surface of the adsorbent. When pH>PZC, the quantity of MB adsorbed by clays increased slightly due to the electrostatic attraction of the positive charge carried by the MB molecule and the negative surface of the adsorbent [21].

2.3. Effect of Contact Time

The adsorbent-adsorbate contact time is an important parameter to understand the adsorption process. This parameter was studied using an initial MB concentration of 100 mg.L^{-1}, while the adsorbents masses were 2, 4, and 6 g.L^{-1} for RC, GC and WC, respectively, with contact times between 5 and 240 min. The results obtained are presented in Figure 8. The retention of MB by the adsorbents was rapid in the first few minutes but became slower and slower over time until equilibrium was established. The initial increase in the adsorption rate can be attributed to a large number of vacant sites available at the beginning [24]. The equilibrium adsorbent-adsorbate times were 30, 45, and 60 min for RC, GC and WC.

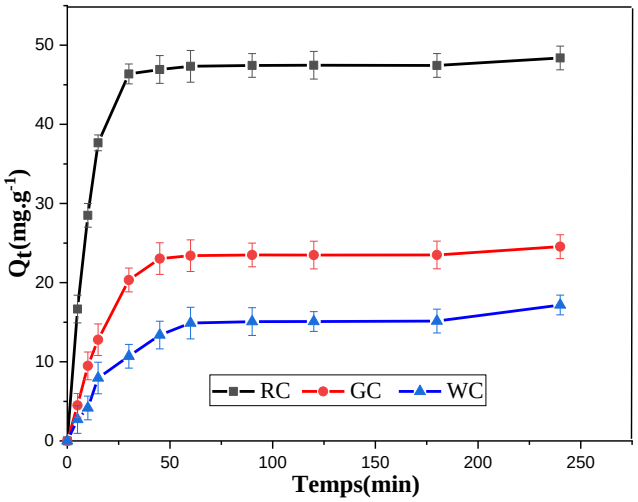

Figure 8. Effect of contact time on the adsorption of MB by RC, GC and WC.

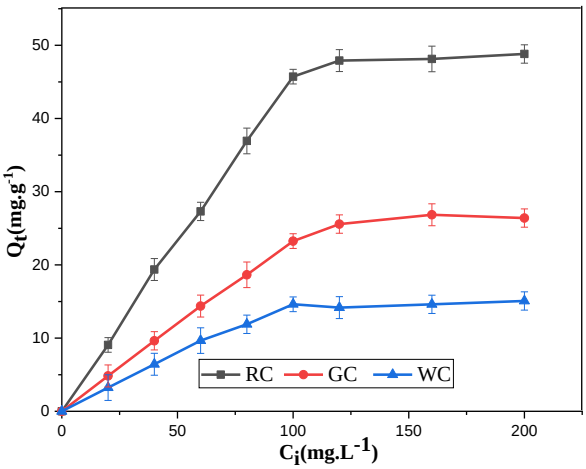

Figure 9. Effect of initial concentration on the adsorption of MB by RC, GC and WC.

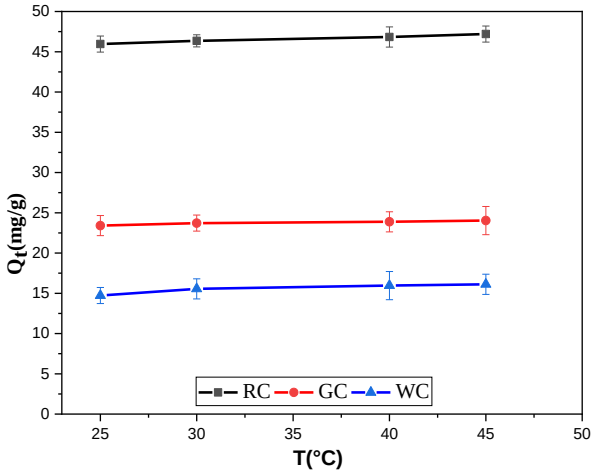

Figure 10. Effect of temperature on the adsorption of MB by RC, GC and WC.

2.4. Effect of Initial Concentration

The influence of the initial concentration of the MB solution on its adsorption by RC, GC, and WC is illustrated in Figure 9. The results show that when the concentration of the pollutant increased from 20 to 200 mg.L^{-1}, the amount of adsorbed dye increased from 9.06 to 45.72 mg.g^{-1} for RC, 4.83 to 23.618 mg.g^{-1} for GC and 3.23 to 14.62 mg.g^{-1} for WC. This increase in initial concentration results in a higher mass transfer by the driving force, which allows greater MB adsorption [32]. Above 100 mg.L^{-1}, the adsorption capacity becomes constant due to saturation of the adsorbent [21].

2.5. Temperature Effects

The influence of temperature is presented in Figure 10. From this figure, we can see a small increase in the quantity of MB adsorbed by RC, GC and WC. This increase can be explained by the movement and dispersion of the adsorbate molecules due to thermal agitation [35].

2.6. Kinetic Study

Three kinetic models (PSO, PFO, and IPD) were used to determine the mechanism of adsorption of MB by the adsorbents. These kinetic models are presented in Figure 11. Based on these figures, the model which best explained the retention of MB by RC, GC and WC was the PSO model. The kinetic parameters of these models and their correlation coefficients are shown in Table 2. It can be seen that the correlation coefficients (R^2) obtained for the PSO model were higher compared to those of the PFO models, while the maximum quantities adsorbed obtained experimentally and by calculation using the PSO model are very close. This confirms that the most suitable model was PSO.

The IPD model was used to study the different steps of the dye adsorption process on the RC, GC and WC samples. Figure 11(c) shows multi-linearity, which suggests that the retention of MB by RC, GC and WC can be described in three steps (Figure 12). First: the transfer of MB molecules from the aqueous solution

to the outer surface of RC, GC and WC (film diffusion); second: the transfer of MB molecules from the outer surface to the inner pores of RC, GC and WC; and third: adsorption of MB molecules on the surface of the RC, GC and WC samples [37]. The values of the K_{in} rate constants, as well as those of R^2 in the table shows that the K_1 values for RC, GC and WC were significantly higher compared to K_2 and K_3, suggesting that the transfer to the outer surface (film diffusion) was the dominant step.

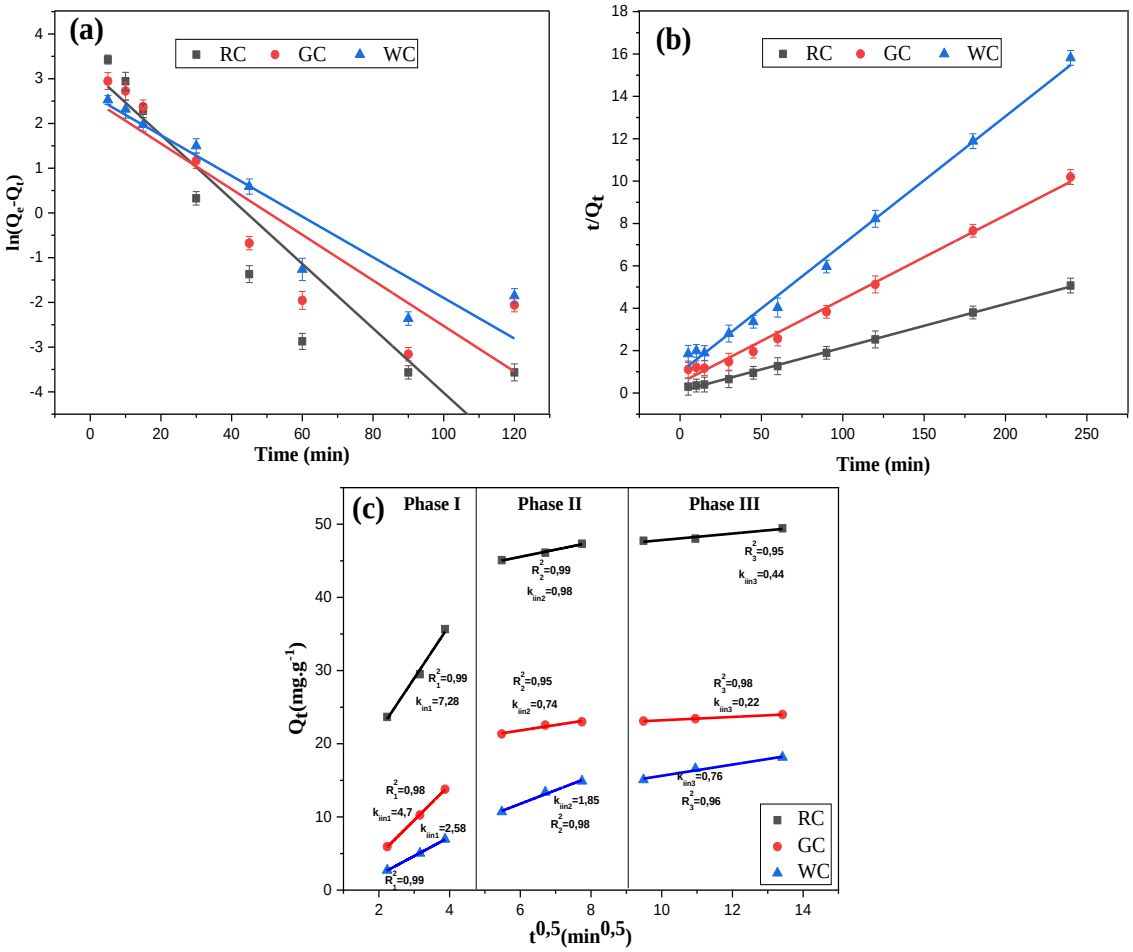

Figure 11. Kinetic models for the adsorption of MB by RC, GC and WC : (a) PFO, (b) PSO and (c) IPD.

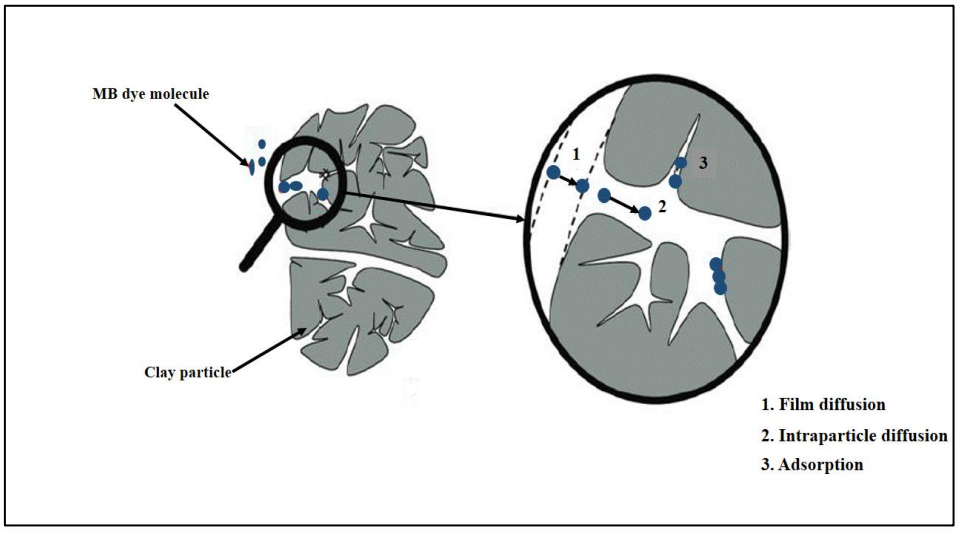

Figure 12. Proposed steps for removal of MB dye using RC, GC and WC.

Table 2. Kinetic parameters for the adsorption of MB by RC, GC and WC.

Clay	Q_{exp} (mg.g^{-1})	Pseudo-first order				Pseudo-second order				Intraparticle diffusion		
		K_1 (min^{-1})	R^2	Q_e (mg.g^{-1})	P	K_2 (g.mg^{-1}.min^{1})	Q_e (mg.g^{-1})	R^2	P	K_{in1}	K_{in2}	K_{in3}
RC	48.63	0.072	0.889	24.17	0.007	0.0050	48.56	0.998	0.002	7.28	0.98	0.44
GC	23.43	0.050	0.804	13.05	0.01	0.00301	25.31	0.992	0.004	4.7	0.74	0.22
WC	15.07	0.045	0.919	14.08	0.006	0.004	16.55	0.993	0.005	2.58	1.85	0.76

2.7. Adsorption Isotherm

The adsorption isotherms of MB by RC, GC and WC were analyzed according to the Langmuir and Freundlich models. Figure 13 shows the adsorption isotherms of MB on the three adsorbents. The parameters and constants characterizing each of the isotherms are listed in Table 3. The Langmuir model showed higher correlation coefficients (R^2) compared to the Freundlich model for all three adsorbents, which indicates the adsorption process of the MB dye on the three adsorbents occurred in a monolayer. The maximum monolayer adsorption capacities were 51.28, 32.46, and 16.31 mg.g^{-1} respectively for RC, GC and WC. The high adsorption capacities for RC and GC compared to WC can be explained by their high CEC values and low CaO content.

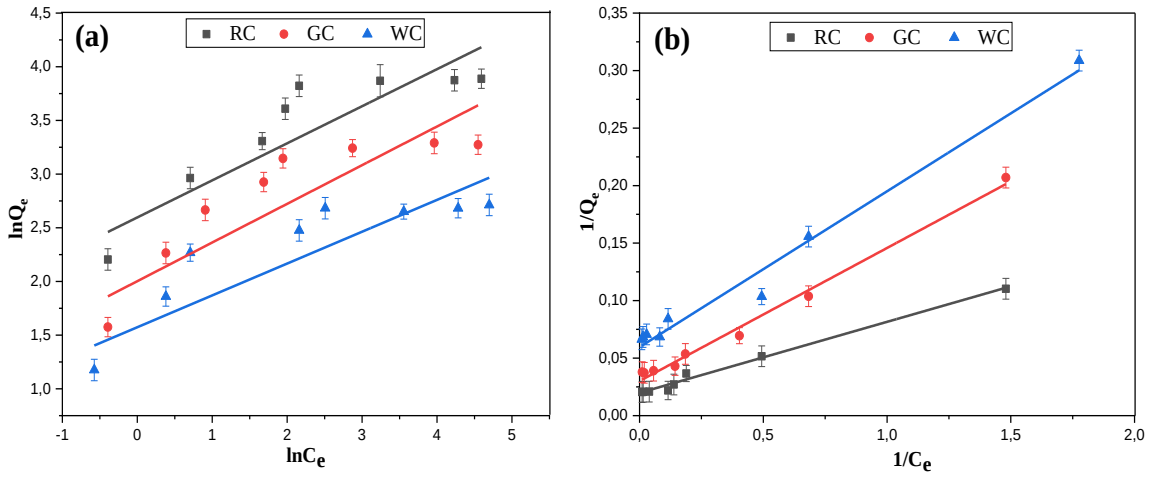

Figure 13. Adsorption isotherms for MB on RC, GC and WC obtained by (a) Freundlich and (b) Langmuir isotherm models.

Table 3. Freundlich and Langmuir isotherm model constants.

Clay	Langmuir constants				Freundlich constants			
	Q_{max} (mg.g^{-1})	K_L (L.g^{-1})	R^2	p	K_F (mg.g^{-1})	1/n	R^2	p
RC	50.47	0.32	0.987	0.004	13.41	0.34	0.819	0.009
GC	32,57	0.26	0.998	0.003	7.41	0.36	0.812	0.01
WC	16.78	0.44	0.971	0.005	4.82	0.29	0.845	0.007

Table 4. Thermodynamic parameters for the adsorption of MB using RC, GC and WC.

Clay	ΔG° (J.mol^{-1})				ΔS° (J.mol^{-1}.K^{-1})	ΔH° (KJ.mol^{-1})
	Temperature (K)					
	298	303	313	318		
RC	-6023.06 ± 52.1	-6405.26 ± 48.1	-7011.23 ± 48.1	-7470.09 ± 39.23	-70.01 ± 0.05	14.32 ± 0.098
GC	-3227.09 ± 18	-3865.56 ± 28.6	-4349.35 ± 26.9	-4843.60 ± 33.7	-73.91 ± 0.062	18.69 ± 0.110
WC	-576.11 ± 6.2	-2123.8 ± 15.41	-3435.12 ± 17.6	-4191.89 ± 41	-170.85 ± 0.12	50.02 ± 0.15

2.8. Thermodynamic Study

The values of the thermodynamic parameters are recorded in Table 4. The negative values of ΔG° indicate that the retention of MB by RC, GC and WC was a spontaneous and thermodynamically favourable process [9]. The positive values of ΔH° for the three adsorbents indicate that the interaction of MB with RC, GC, and WC was an endothermic process [21]. The negative value of ΔS° obtained for the used clays indicates that the MB molecules were more organized at the solid/liquid interface than in the liquid phase [19].

2.9. Regeneration of RC, GC and WC

Regeneration allows the recycling of spent adsorbents by several methods including chemical regeneration, oxidation regeneration, microwave regeneration, thermal regeneration, and other techniques [38]. In this study, the regeneration of RC, GC and WC was realized by a thermal method. The results obtained are shown in Figure 14. After five cycles of regeneration, the desorption efficiency of MB decreased from 95 % to 65 % for RC, 93 % to 58 % for GC, and 90 % to 24 % for WC. This decrease can be explained by the occupation of the active sites during recycling.

2.10. Comparative Study

Table 5 compares the adsorption capacities of RC, GC and WC we obtained with the results of other studies. The results achieved in this study show that the removal capacities of these adsorbents were higher than other adsorbents. Moreover, the adsorbents used here were abundant in nature, less costly, and easy to separate.

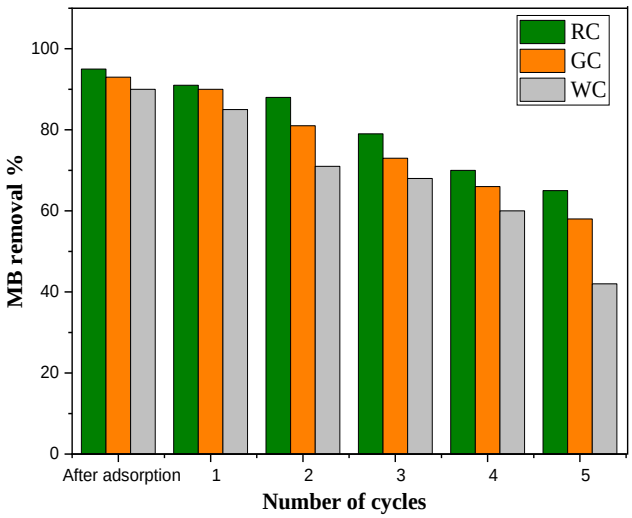

Figure 14. Regeneration of RC, GC and WC.

Table 5. Comparison of MB adsorption using different adsorbents.

Adsorbents	Q_{max} (mg.g^{-1})	Reference
NaOH-treated raw kaolin	16.34	[39]
Raw kaolin	13.99	[39]
Red-clay	18.83	[5]
Fly ash-derived zéolites	12.64	[40]
Phosphoric acid-based géopolymères	4.26	[41]
Zeolite	8.67	[42]
SDBS-modified zéolite	15.68	[42]
Montmorillonite-rich Moroccan clay	25.01	[32]
Activated carbon prepared from rice husks	14.34	[43]
rice husks	9.83	[43]
Moroccan Illitic	13.60	[28]
RC	50.47	Present study
GC	32,57	
WC	16.78	

CONCLUSION

The RC, GC and WC samples in this study were successfully used for the removal of MB from an aqueous solution. The FTIR spectra obtained before and after the process confirmed the adsorption of MB by these clay samples. The adsorption capacities of RC, GC and WC were significant in the basic medium. The kinetic study revealed that the adsorption mechanism was best described by the PSO model, while the adsorption isotherms for the three clays were well approximated by the Langmuir model. The maximum adsorption capacity of RC was higher than those of GC and WC. The adsorption process was endothermic and thermodynamically favourable for all three clay samples. However, the percentage removal of MB decreased during recycling. This study concluded that the use of raw clays was a low-cost option for textile effluent treatment. This work opens new perspectives for the studied materials. Adsorption capacity is an important parameter that may be explored and improved by chemical or thermal modification and synthesis of new materials based on these clays, such as geopolymers. Thus, they have good potential for application in the treatment of media contaminated by heavy metals and other organic pollutants such as pesticides and pharmaceuticals. More studies need to be done to evaluate how these materials may be used at the industrial scale in effluent treatment plants.

CONFLICT OF INTEREST

Authors report no conflict of interest.

REFERENCES

1. Ramezani, F., Zare-Dorabei, R. (2019) Simultaneous ultrasonic-assisted removal of malachite green and methylene blue from aqueous solution by Zr-SBA-15. *Polyhedron*, **166**, 153–61.

2. Elmoubarki, R., Mahjoubi, F. Z., Tounsadi, H., Moustadraf, J., Abdennouri, M., Zouhri, A., et al. (2015) Adsorption of textile dyes on raw and decanted Moroccan clays: Kinetics, equilibrium and thermodynamics. *Water Resour Ind.*, **9**, 16–29.

3. Tuli, F. J., Hossain, A., Kibria, A. K. M. F., Tareq, A. R. M., Mamun, S. M. M. A., Ullah, A. K. M. A. (2020) Removal of methylene blue from water by low-cost activated carbon prepared from tea waste: A study of adsorption isotherm and kinetics. *Environ Nanotechnol Monit Manag*., **14**, 100354.

4. Setiabudi, H. D., Jusoh, R., Suhaimi, S. F. R. M., Masrur, S. F. (2016) Adsorption of methylene blue onto oil palm (Elaeis guineensis) leaves: Process optimization, isotherm, kinetics and thermodynamic studies. *J Taiwan Inst Chem Eng.*, **63**, 363–70.

5. Bentahar, Y., Draoui, K., Hurel, C., Ajouyed, O., Khairoun, S., Marmier, N. (2019) Physico-chemical characterization and valorization of swelling and non-swelling Moroccan clays in basic dye removal from aqueous solutions. *J Afr Earth Sci.*, **154**, 80–88.

6. Sana, D., Jalila, S. (2017) A comparative study of adsorption and regeneration with different agricultural wastes as adsorbents for the removal of methylene blue from aqueous solution. *Chin J Chem Eng*., **25**, 1282–1287.

7. Song, J., Zou, W., Bian, Y., Su, F., Han, R. (2011) Adsorption characteristics of methylene blue by peanut husk in batch and column modes. *Desalination*, **265**, 119–125.

8. Mouni, L., Belkhiri, L., Bollinger, J. -C., Bouzaza, A., Assadi, A., Tirri, A., et al. (2018) Removal of Methylene Blue from aqueous solutions by adsorption on Kaolin: Kinetic and equilibrium studies. *Appl Clay Sci*., **153**, 38–45.

9. Saufi, H., Alouani, M. E., Aride, J., Taibi, M. (2020) Rhodamine B biosorption from aqueous solution using Eichhornia crassipes powders: Isotherm, kinetic and thermodynamic studies. *Chem Data Collect*, **25**, 100330.

10. Dali Youcef, L., Belaroui, L. S., López-Galindo, A. (2019) Adsorption of a cationic methylene blue dye on an Algerian palygorskite. *Appl Clay Sci*., **179**, 105145.

11. Almeida, C. A. P., Debacher, N. A., Downs, A. J., Cottet, L., Mello, C. A. D. (2009) Removal of methylene blue from colored effluents by adsorption on montmorillonite clay. *J Colloid Interface Sci*., **332**, 46–53.

12. Miyoshi, Y., Tsukimura, K., Morimoto, K., Suzuki, M., Takagi, T. (2018) Comparison of methylene blue adsorption on bentonite measured using the spot and colorimetric methods. *Appl Clay Sci.*, **151**, 140–147.

13. Rida, K., Bouraoui, S., Hadnine, S. (2013) Adsorption of methylene blue from aqueous solution by kaolin and zeolite. *Appl Clay Sci.*, 83–84, 99–105.

14. Azejjel, H., del Hoyo, C., Draoui, K., Rodríguez-Cruz, M. S., Sánchez-Martín, M. J. (2009) Natural and modified clays from Morocco as sorbents of ionizable herbicides in aqueous medium. *Desalination*, **249**, 1151–1158.

15. Bentahar, Y., Hurel, C., Draoui, K., Khairoun, S., Marmier, N. (2016) Adsorptive properties of Moroccan clays for the removal of arsenic (V) from aqueous solution. *Appl Clay Sci.*, **119**, 385–392.

16. Deehmani, Y., Sellaoui, L., Alghamdi, Y., Lainé, J., Badawi, M., Amhoud, A., et al. (2020) Kinetic, thermodynamic and mechanism study of the adsorption of phenol on Moroccan clay. *J Mol Liq*., **312**, 113383.

17. Dalvand, A., Nabizadeh, R., Reza Ganjali, M., Khoobi, M., Nazmara, S., Hossein Mahvi, A. (2016) Modeling of Reactive Blue 19 azo dye removal from colored textile wastewater using L-arginine-functionalized Fe3O4 nanoparticles: Optimization, reusability, kinetic and equilibrium studies. *J Magn Magn Mater.*, **404**, 179–189.

18. Aran, D., Maul, A., Masfaraud, J. -F. (2008) A spectrophotometric measurement of soil cation exchange capacity based on cobaltihexamine chloride absorbance. *Comptes Rendus Geosci*., **340**, 865–871.

19. Bassam, R., El hallaoui, A., El Alouani, M., Jabrane, M., El Khattabi, E. H., Tridane, M., et al. (2021) Studies on the Removal of Cadmium Toxic Metal Ions by Natural Clays from Aqueous Solution by Adsorption Process. Singh AK, editor. *J Chem.*, 1–14.

20. Sousa, H. R., Silva, L. S., Sousa, P. A. A., Sousa, R. R. M., Fonseca, M. G., Osajima, J. A., et al. (2019) Evaluation of methylene blue removal by plasma activated palygorskites. *J Mater Res Technol.*, **8**, 5432–5442.

21. He, Y., Zhang, L., An, X., Wan, G., Zhu, W., Luo, Y. (2019) Enhanced fluoride removal from water by rare earth (La and Ce) modified alumina: Adsorption isotherms, kinetics, thermodynamics and mechanism. *Sci Total Environ*., **688**, 184–198.

22. Abdullah, A. H. D., Chalimah, S., Primadona, I., Hanantyo, M. H. G. (2018) Physical and chemical properties of corn, cassava, and potato starchs. *IOP Conf Ser Earth Environ Sci*., **160**, 012003.

23. El Alouani, M., Alehyen, S., El Achouri, M., Taibi, M. (2019) Comparative study of the adsorption of micropollutant contained in aqueous phase using coal fly ash and activated coal fly ash: Kinetic and isotherm studies. *Chem Data Collect*., **23**, 100265.

24. Sakin Omer, O., Hussein, M. A., Hussein, B. H. M., Mgaidi, A. (2018) Adsorption thermodynamics of cationic dyes (methylene blue and crystal violet) to a natural clay mineral from aqueous solution between 293.15 and 323.15 K. *Arab J Chem*., **11**, 615–623.

25. Rahmani, S., Zeynizadeh, B., Karami, S. (2020) Removal of cationic methylene blue dye using magnetic and anionic-cationic modified montmorillonite: kinetic, isotherm and thermodynamic studies. *Appl Clay Sci.*, **184**, 105391.

26. Alouani, M. E., Alehyen, S., Achouri, M. E., M'hamed Taibi (2019) Comparative Studies on Removal of Textile Dye onto Geopolymeric Adsorbents. EnvironmentAsia. *Thai Society of*

Higher Education Institutes on Environment, **12**, 143153.

27. Kannan, S. (2014) FT-IR and EDS analysis of the seaweeds Sargassum wightii (brown algae) and Gracilaria corticata (red algae), **11**.

28. Jawad, A. H., Abdulhameed, A. S. (2020) Mesoporous Iraqi red kaolin clay as an efficient adsorbent for methylene blue dye: Adsorption kinetic, isotherm and mechanism study. *Surf Interfaces*, **18**, 100422.

29. Li, Z., Chang, P. -H., Jiang, W. -T., Jean, J. -S., Hong, H. (2011) Mechanism of methylene blue removal from water by swelling clays. *Chem Eng J.*, **168**, 1193–200.

30. El Alouani, M., Alehyen, S., El Achouri, M., Taibi, M. (2019) Preparation, Characterization, and Application of Metakaolin-Based Geopolymer for Removal of Methylene Blue from Aqueous Solution. *J Chem.*, **2019**, 1–14.

31. Zerzouri Lakhssassi, M., Alehyen, S., El Alouani, M., Taibi, M. (2019) The effect of aggressive environments on the properties of a low calcium fly ash based geopolymer and the ordinary Portland cement pastes. *Mater Today Proc.*, **13**, 1169–1177.

32. Alouani, M. E., Alehyen, S., Zerzouri, M., Achouri, M. E., Taibi, M. (2019) Enhancing the Removal of Organic Pollutant-Methylene Blue-by a Morroccan Natural Clay, **13**.

33. Elmoubarki, R., Taoufik, M., Moufti, A., Elhalil, A., Mahjoubi, F. Z., Abdennouri, M., et al. (2020) Color and organic matter removal from textile effluents by synthetic layered double hydroxides and natural clays. J Appl Surf Interfaces. *Journal of Applied Surfaces and Interfaces*, **6**, 13 (2019).

34. Hao, W., Flynn, S. L., Alessi, D. S., Konhauser, K. O. (2018) Change of the point of zero net proton charge (pHPZNPC) of clay minerals with ionic strength. *Chem Geol.*, **493**, 458–467.

35. Miyah, Y., Lahrichi, A., Idrissi, M., Khalil, A., Zerrouq, F. (2018) Adsorption of methylene blue dye from aqueous solutions onto walnut shells powder: Equilibrium and kinetic studies. *Surf Interfaces*, **11**, 74–81.

36. Machrouhi, A., Elhalil, A., Farnane, M., Mahjoubi, F. Z., Tounsadi, H., Sadiq, M., et al. (2017) Adsorption behavior of methylene blue onto powdered Ziziphus lotus fruit peels and Avocado kernels seeds. *J Appl Surf Interfaces. Journal of Applied Surfaces and Interfaces*, **1**, 13 (2017).

37. El Alouani, M., Alehyen, S., El Hadki, H., Saufi, H., Elhalil, A., Kabbaj, O. K., et al. (2021) Synergetic influence between adsorption and photodegradation of Rhodamine B using synthesized fly ash based inorganic polymer. *Surf Interfaces*, **24**, 101136.

38. Momina, M., Shahadat, M., Isamil, S. (2018) Regeneration performance of clay-based adsorbents for the removal of industrial dyes: a review. *RSC Adv.*, **8**, 24571–24587.

39. Ghosh, D., Bhattacharyya, K. G. (2002) Adsorption of methylene blue on kaolinite. *Appl Clay Sci.*, **20**, 295–300.

40. Woolard, C. D., Strong, J., Erasmus, C. R. (2002) Evaluation of the use of modified coal ash as a potential sorbent for organic waste streams. *Appl Geochem.*, **17**, 1159–1164.

41. Khan, M. I., Min Teoh, K., Azizli, K., Sufian, S., Ullah, H., Man, Z. (2015) Effective removal of methylene blue from water using phosphoric acid based geopolymers: synthesis, characterizations and adsorption studies. *RSC Adv.*, **5**, 61410–61420.

42. Jin, X., Jiang, M., Shan, X., Pei, Z., Chen, Z. (2008) Adsorption of methylene blue and orange II onto unmodified and surfactant-modified zeolite. *J Colloid Interface Sci.*, **328**, 243–247.

43. Sharma, Y. C., Uma (2010) Optimization of Parameters for Adsorption of Methylene Blue on a Low-Cost Activated Carbon. *J Chem Eng Data*, **55**, 435–439.